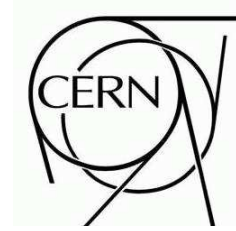




# ATLAS NOTE

September 30, 2009



Kinematic fitting of  $t\bar{t}$  events using a likelihood approach –  
The KLFFitter package

Johannes Erdmann, Kevin Kröninger  
Olaf Nackenhorst, Arnulf Quadt

II. Institute of Physics  
Georg-August-Universität Göttingen

## Abstract

A software package for the reconstruction of semi-leptonic  $t\bar{t}$  events is presented. It is based on a likelihood approach where an emphasis is placed on the description of the energy resolution of jets.

# 1 Introduction

This note describes a tool for kinematic fitting [1]. It is based on a likelihood approach with an emphasis on the (non-Gaussian) description of the energy resolution of the objects in the final state. The tool is general and its features are described for the example of semi-leptonic  $t\bar{t}$ -events (more specifically, the electron plus jets channel).

The semi-leptonic  $t\bar{t}$ -decay results in four quarks, a high- $p_T$  lepton (here: electron) and missing transverse energy in the final state of the hard scattering process. The four quarks are detected as exactly four jets only if no jet is lost (e.g., if a jet lies outside the acceptance region or does not pass the minimum selection criteria) and if no additional initial or final state radiation (ISR/FSR) is present. In this case there are 24 possible jet permutations for which jets can be associated with quarks from the final state. Since the two quarks from the decay of one of the W bosons are indistinguishable only twelve permutations remain. All but the correct permutation are referred to as combinatorial background. This definition also includes permutations in which not all jets come from one of the four final state quarks but from ISR/FSR.

The studies presented in this note aim to estimate the efficiency of partially or fully identifying top quarks and to estimate the improvement in energy resolution.

First, the kinematic fitting approach is introduced. The Monte Carlo data samples used for this study and the event selection are described in section 3. The parameterization of the energy resolution used in this study and the derivation of the relevant parameters are discussed in section 4. The results are summarized in section 5. Subsequently, a short summary and an outlook are given.

## 2 Kinematic fitting of semi-leptonic $t\bar{t}$ events

The kinematic fitting is done using a likelihood approach. The likelihood is defined as the probability for observing a set of measured quantities given a model and a corresponding set of model parameters. The probability is calculated according to the model, in this case assuming the event under study is a semi-leptonic  $t\bar{t}$  event. The final state of the (leading order) decay comprises of four quarks, one charged lepton and the corresponding (anti-)neutrino. The quarks are two light quarks from the hadronically decaying W boson and two b quarks from the decay of the two top quarks.

The quantities which are used from the measurement are

- the energies and directions of four jets associated with the  $t\bar{t}$ -system,  $\tilde{E}_i, \tilde{\Omega}_i = (\eta_i, \phi_i)$ ;
- the energy and direction of the charged lepton,  $\tilde{E}_{\text{lep}}, \tilde{\Omega}_{\text{lep}}$ ;
- the missing transverse energy,  $E_T^{\text{miss}}$ .

The direction of the charged lepton is assumed to be measured precisely. The energies of the quarks and the charged lepton as well as the directions of the four quarks are only known with some uncertainty given by the corresponding energy and angular resolution. These resolutions are parametrized by *transfer functions*,  $W(\tilde{E}_i, E_i)$ , which map the measured energy of an object

to the energy of the final state particles, and  $W(\tilde{\Omega}_i, \Omega_i)$ , which map the measured angles of an object to the angles of the final state particles. The parametrization is discussed in section 4. Since neutrinos do not interact with the detector the momentum of the neutrino cannot be measured directly, but its transverse momentum can be estimated from the missing transverse momentum in the event. Hence, transfer functions for the  $x$  and  $y$  components of the neutrino momentum,  $W(E_{x/y}^{\text{miss}}, p_{x/y}^\nu)$ , can be defined.

The calculation of the Likelihood is based on the following assumptions:

1. the transfer functions  $W(\tilde{E}, E)$  of all quark and the charged lepton energies are known;
2. the transfer functions  $W(\tilde{\Omega}, \Omega) = W(\tilde{\eta}, \eta) \cdot W(\tilde{\phi}, \phi)$  of all quark angles are known;
3. the transfer functions  $W(E_{x/y}^{\text{miss}}, p_{x/y}^\nu)$  of the neutrino momentum are known;
4. the mass of the hadronically and leptonically decaying  $W$  boson,  $m_{jj}$  and  $m_{e\nu}$ , respectively, are distributed according to a Breit-Wigner distribution around a pole mass of  $M_W = 80.4 \text{ GeV}/c^2$ ;
5. the masses of the two top quarks,  $m_{jjj}$  and  $m_{e\nu j}$ , are distributed according to a Breit-Wigner distribution around the top pole mass. The pole mass is either an additional free parameter or fixed to the top pole mass used in the generation of the Monte Carlo events or, in data, to a value from previous measurements.

The parameters used in the fitting procedure are

- the energies and directions of the four quarks,  $E_i, \Omega_i$  ( $3 \times 4 = 12$  parameters);
- the energy and direction of the charged lepton,  $E_l$  (1 parameter);
- the momentum of the neutrino,  $\vec{p}^\nu$  (3 parameters);
- (optional) the top pole mass,  $M_{\text{top}}$  (1 parameter).

The parameter ranges are set individually for each event. The energies of the partons and the charged lepton have to be within a certain range around the measured values ( $\min(0, \tilde{E} - n \cdot \sqrt{\tilde{E}}) < E < \tilde{E} + n \cdot \sqrt{\tilde{E}}$ , where  $n = 7$  for jets/partons and  $n = 2$  for electrons). The  $z$ -component of the neutrino momentum has to be within a range of  $\pm 1 \text{ TeV}/c$ . The  $x$ - and  $y$ -components of the neutrino momentum have to be within a range of  $\pm 100 \text{ GeV}$  around the measured components of the missing transverse energy. The  $\eta$ - and  $\phi$ -angles of the jets have to be within a range of  $\pm 0.2$  and  $\pm 0.1$  around the measured values, respectively. The top pole mass is constrained to be between  $100 \text{ GeV}/c^2$  and  $400 \text{ GeV}/c^2$ .

The likelihood function is

$$L = \left( \prod_{i=1}^4 W(\tilde{E}_i, E_i) \right) \cdot W(\tilde{E}_l, E_l) \cdot W(E_x^{\text{miss}} | p_x^\nu) \cdot W(E_y^{\text{miss}} | p_y^\nu) \cdot \left( \prod_{i=1}^4 W(\tilde{\Omega}_i | \Omega_i) \right) \cdot BW(m_{jj} | M_W) \cdot BW(m_{e\nu} | M_W) \cdot BW(m_{jjj} | M_{\text{top}}) \cdot BW(m_{e\nu j} | M_{\text{top}}),$$

where  $BW(x|y)$  is a Breit-Wigner function centered around  $y$ .

An *a priori* association of jets with quarks is not possible. Thus, all possible ways to associate jets with quarks have to be taken into account. Since the Likelihood is symmetric under the permutation of the two jets associated with the two quarks from the hadronically decaying  $W$ -boson, only twelve (out of 24) permutations of jets are taken into account. Each permutation can be weighted with  $b$ -tagging weights. This feature is implemented but not used in the initial version of the fitter. Permutations for which the invariant mass of the jets associated with the two light quarks are not within a range of  $40 \text{ GeV}/c^2$ – $120 \text{ GeV}/c^2$  are excluded from the fit. For the moment, permutations for which a minimum could not be found were also disregarded. Less than 1% of the events were affected.

The function  $-\ln L$  is then minimized with respect to the parameters for each permutation. The modelling is done using the BAT package [2] where the minimization is done with the interface to Minuit. The starting values for the energies, the invariant masses and the angles are the measured values. The  $z$ -component of the neutrino momentum is calculated from the initial values and the solution giving the larger Likelihood is used as starting value.

The fitter returns (i) the best fit parameters, (ii) the corresponding value of the likelihood, referred to as  $-\ln L^*$  in the following, and (iii) a relative weight for each jet permutation. The weights are built from  $\ln L^*$  and the  $b$ -tagging weights such that the sum of relative weights is normalized to unity. The permutations are ordered according to their relative weight.

### 3 Monte Carlo data sample and event selection

The studies presented in this note are performed on a Monte Carlo data sample containing events with di-leptonic and semi-leptonic final states (`r635_t53`). The events were generated with MC@NLO at a centre-of-mass energy of 10 TeV and a top pole mass of  $172.5 \text{ GeV}/c^2$ . The total number of events in the sample is roughly 2.25 million. The events were passed to the ATLAS simulation software and reconstructed using Athena 14.2.25. The final Root-tuple was created using GoTopTree 01-01-04.

The following object definitions are used

- medium electrons with  $p_T > 15 \text{ GeV}/c$  and  $|\eta| < 2.47$  (excluding the crack-region);
- H1 calibrated tower cone jets with a cone size of 0.4, and  $p_T > 15 \text{ GeV}/c$  and  $|\eta| < 2.5$ ;
- missing  $E_T$  defined as MET\_RefFinal.

Jets overlapping with electrons are removed if their distance in  $\eta - \phi$ -space is  $\Delta R = \sqrt{\Delta\phi^2 + \Delta\eta^2} < 0.2$ .

#### 3.1 Pre-selection

Only events in the semi-leptonic decay channel with electrons in the final state ( $e$ +jets) are considered in the following. A pre-selection on truth level is applied. All events are required to have exactly one electron (and no tau), two  $b$  quarks and two light quarks in the truth container. 625,892 events fulfill this requirement. In addition the event are required to have at least one electron and one jet. This leaves 332,159 events which pass the pre-selection.

### 3.2 Event selection

The event selection criteria are similar to those in the CSC-notes [3]. The criteria and a cut flow are shown in Tab. 1. 124,564 events pass the cuts. The four leading jets (in  $p_T$ ) are associated with the  $t\bar{t}$ -system and used for the evaluation of the likelihood. All other jets are ignored.

Table 1: Cut flow for the event selection and matching.  $N_{\text{ev}}$  is the number of events remaining after the cut.  $\epsilon_{\text{rel}}$  is the relative efficiency with respect to the number of events after the previous cut.  $\epsilon_{\text{abs}}$  is the efficiency with respect to the pre-selected sample size.

Cut	$N_{\text{ev}}$	$\epsilon_{\text{rel}}$	$\epsilon_{\text{abs.}}$
Pre-selected sample	332,159	1.00	1.00
1 electron with $p_T > 20$ GeV/c and $ \eta  < 2.5$	310,078	0.93	0.93
3 jets with $p_T > 40$ GeV/c and $ \eta  < 2.5$ , and $\geq 1$ add. jet with $p_T > 20$ GeV/c and $ \eta  < 2.5$	140,396	0.45	0.42
$E_T^{\text{miss}} \geq 20$ GeV	124,564	0.89	0.38
1 matched electron with $\Delta R \leq 0.3$	123,384	1.00	0.37
4 matched quarks with $\Delta R \leq 0.3$	27,163	0.22	0.08

### 3.3 Matching

For some of the studies performed it is important to identify jets with the corresponding quarks from the (leading order) hard scattering process. This identification is done by requiring a geometric matching criterion based on their distance in  $\eta - \phi$ -space. This difference is defined as  $\Delta R = \sqrt{\Delta\eta^2 + \Delta\phi^2}$ , where  $\Delta\eta$  and  $\Delta\phi$  are the differences between the two objects in  $\eta$  and  $\phi$ , respectively. Two objects are *matched* if  $\Delta R < 0.3$ . Based on this definition, an event is referred to as matched if the four selected jets in the event are matched to the four partons in the final state of the hard scattering process and if the lepton candidate is matched to the truth lepton. Table 1 summarizes the number of selected events which fulfill the two requirements. 27,163 matched events are found in the sample.

## 4 Derivation of the transfer functions

The transfer functions used in this analysis are derived from the Monte Carlo sample described in section 3. The  $p_T$ -requirement in the object definition of jets and charged leptons is changed to  $p_T > 7$  GeV/c to minimize any possible bias in the derivation of the energy transfer functions. No further selection is applied to the sample. Transfer functions are derived from reconstructed objects which are matched to the corresponding truth particles using the matching requirement presented in section 3.3.

The transfer functions for the energies depend on the type of the object and the  $\eta$ -region it was found in. The object types distinguished are electrons, light jets and b jets. The  $\eta$ -regions considered are  $(0 < \eta < 1.0)$ ,  $(1 < \eta < 1.7)$  and  $(1.7 < \eta < 2.5)$ , and are motivated by the detector geometry. The energy transfer functions are derived from a two-dimensional binned likelihood fit. One dimension is the energy of the reconstructed object which is subdivided into ten bins with a bin width that is constant in  $\ln E$ . The minimum energy depends on the object and the  $\eta$ -region (again to reduce any possible bias), the maximum is set to 500 GeV. The second dimension is the relative (with respect to the true energy) difference between the

measured and the true energy. The transfer functions are parameterized by double Gaussians. The best-fit parameters can be found in appendix A. The transfer function for the angles and the missing transverse energy are estimated similarly. Further studies on the derivation of the transfer functions, the parameterization and a test of consistency are planned for the near future.

## 5 Results

Studies are performed to show that the approach can help (i) to improve the efficiency of correctly associating jets to quarks, and (ii) to improve the energy resolution of the final state particles. The studies are performed with a fixed top pole mass and repeated without a constraint on the top pole mass. The results are summarized in the following. Distributions of control variables can be found in appendix B. Note that the NLO weight has been used in the calculation of efficiencies and the distributions.

### 5.1 Reconstruction efficiency

The kinematic fitter returns candidate jets associated with the final state quarks in the hard scattering process. The candidates are chosen according to their relative weight. Studies have been performed to estimate the efficiency for finding (i) the correct permutation, (ii) the correct pair of quarks from the hadronically decaying W boson, (iii) the b quark from the hadronically decaying top quark, and (iv) the b quark from the leptonically decaying top quark. The efficiency is estimated as the fraction of events in which the object under study was reconstructed correctly. Only matched events are used in this study. Thus, to be more precise, the efficiency is defined as the probability of finding the correct permutation of jets (out of twelve) given that the jets are the only jets from the  $t\bar{t}$ -system. Table 2 and Fig. 1 summarize these reconstruction efficiencies. The efficiencies to find the correct permutations are 56.36% and 67.67% for the two constraints, respectively. The expected efficiency from combinatorics alone (no kinematic fitting) is 8.33%. The efficiencies for correctly identifying the hadronic W boson and the two b quarks are well above 50% in both cases. As expected, the efficiencies are significantly larger for a fixed top pole mass.

The potential to identify b jets has also been estimated in this study. The quantities of interest are the *b-tagging probability* and the *misidentification probability*, i.e. the probability to associate a jet with a b quark given a b jet,  $p(\text{b-tag}|\text{b jet})$ , *orlightjet*,  $p(\text{b-tag}|\text{lightjet})$ , respectively. These probabilities are summarized in Tab. 2 and Fig. 1. The b-tagging probability is larger than 80% for both constraints whereas the misidentification probability ranges from 15%-19%. Again, fixing the top pole mass improves the performance significantly.

### 5.2 Direction of the top quarks

The direction of the reconstructed top quarks is compared to the direction of the true top quarks in the Monte Carlo. The deviation between the two directions is measured in  $\eta - \phi$ -space. Matching is not required for this study. Figure 2 shows the distributions of  $\log \Delta R$  for the hadronic and leptonic top quarks, respectively, for the two different constraints on the top pole mass (top and bottom). All distributions range from -2.1 to 0.4. A peak at a value of 0.4 and a shoulder at around -1 is visible for non-matched events (dotted line). The peak at 0.4 is

Table 2: Reconstruction efficiencies and probabilities (in %) for pure combinatorics (no kinematic fitting) and the two different constraints on the top pole mass. The label *b-tag* corresponds to the case that a jet is identified as b jet.

Efficiency/ probability	Pure combinatorics	Top pole mass free	Top pole mass fixed
<i>Event-based efficiencies</i>			
$\epsilon(\text{all correct})$	8.33	$56.36 \pm 0.55$	$67.67 \pm 0.61$
$\epsilon(\text{hadronic W correct})$	16.67	$65.58 \pm 0.60$	$71.84 \pm 0.63$
$\epsilon(\text{hadronic b correct})$	25.00	$59.42 \pm 0.57$	$70.10 \pm 0.63$
$\epsilon(\text{leptonic b correct})$	25.00	$76.09 \pm 0.64$	$85.37 \pm 0.69$
<i>Jet-based probabilities</i>			
$p(\text{b-tag} \text{b jet})$	50.00	$81.36 \pm 0.67$	$84.81 \pm 0.69$
$p(\text{b-tag} \text{light jet})$	50.00	$18.64 \pm 0.32$	$15.19 \pm 0.29$

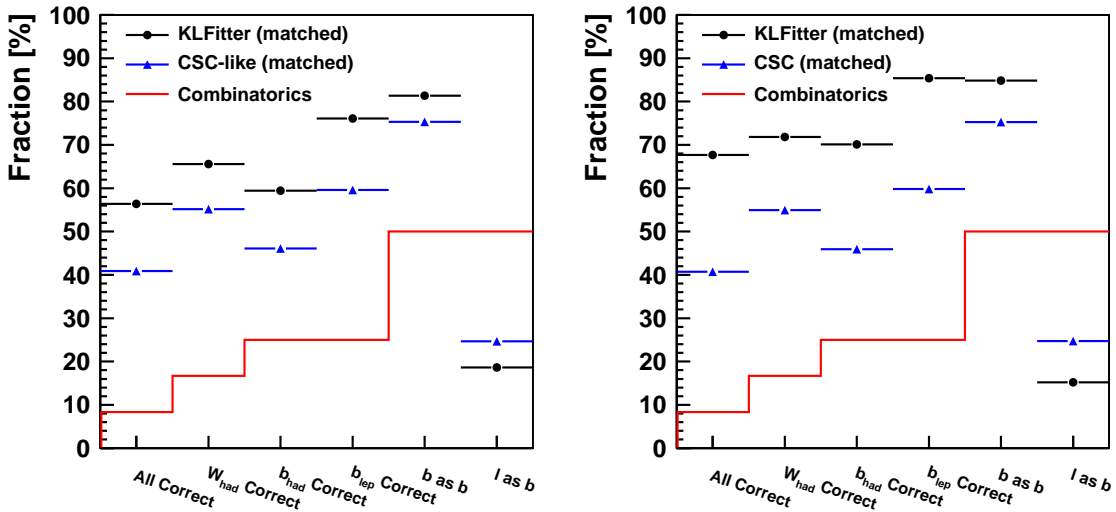


Figure 1: Reconstruction efficiencies and probabilities for pure combinatorics (no kinematic fitting) and the two different constraints (left: top pole mass free, right: top pole mass fixed). The label *l as b* corresponds to the case that a light jet is identified as b jet.

more pronounced in the case of a free top pole mass. It can be explained by the combinatorial background and jets which are falsely associated with the  $t\bar{t}$ -system. The shoulder is also observed in the distributions of matched events and reflects the intrinsic potential of the method to reconstruct the direction of the top quarks. The shoulder is broader for the leptonic top quark since the neutrino momentum is not reconstructed as precisely as the jets in the hadronic system. A small peak at larger values is also visible and associated with combinatorial background alone.

Table 3 summarizes the results. The fraction of events in which  $\Delta R$  is smaller than 0.1, 0.3, and 0.5 are listed for the two different constraints. As expected, the hadronic top quark can be reconstructed more precisely than the leptonic top quark. Fixing the top pole mass improves the reconstruction of the direction of the hadronic and leptonic top quarks.

Table 3: Fraction of events (in %) with a distance between the true and the reconstructed particles of  $\Delta R < 0.1, 0.3, 0.5$ , respectively. for the two constraints. No matching was required.

Fraction of events	Top pole mass free	Top pole mass fixed
<i>Hadronic top quark</i>		
$\Delta R < 0.1$	9.64	11.06
$\Delta R < 0.3$	26.52	29.89
$\Delta R < 0.5$	37.05	41.36
<i>Leptonic top quark</i>		
$\Delta R < 0.1$	6.64	8.08
$\Delta R < 0.3$	22.08	27.14
$\Delta R < 0.5$	32.16	39.60



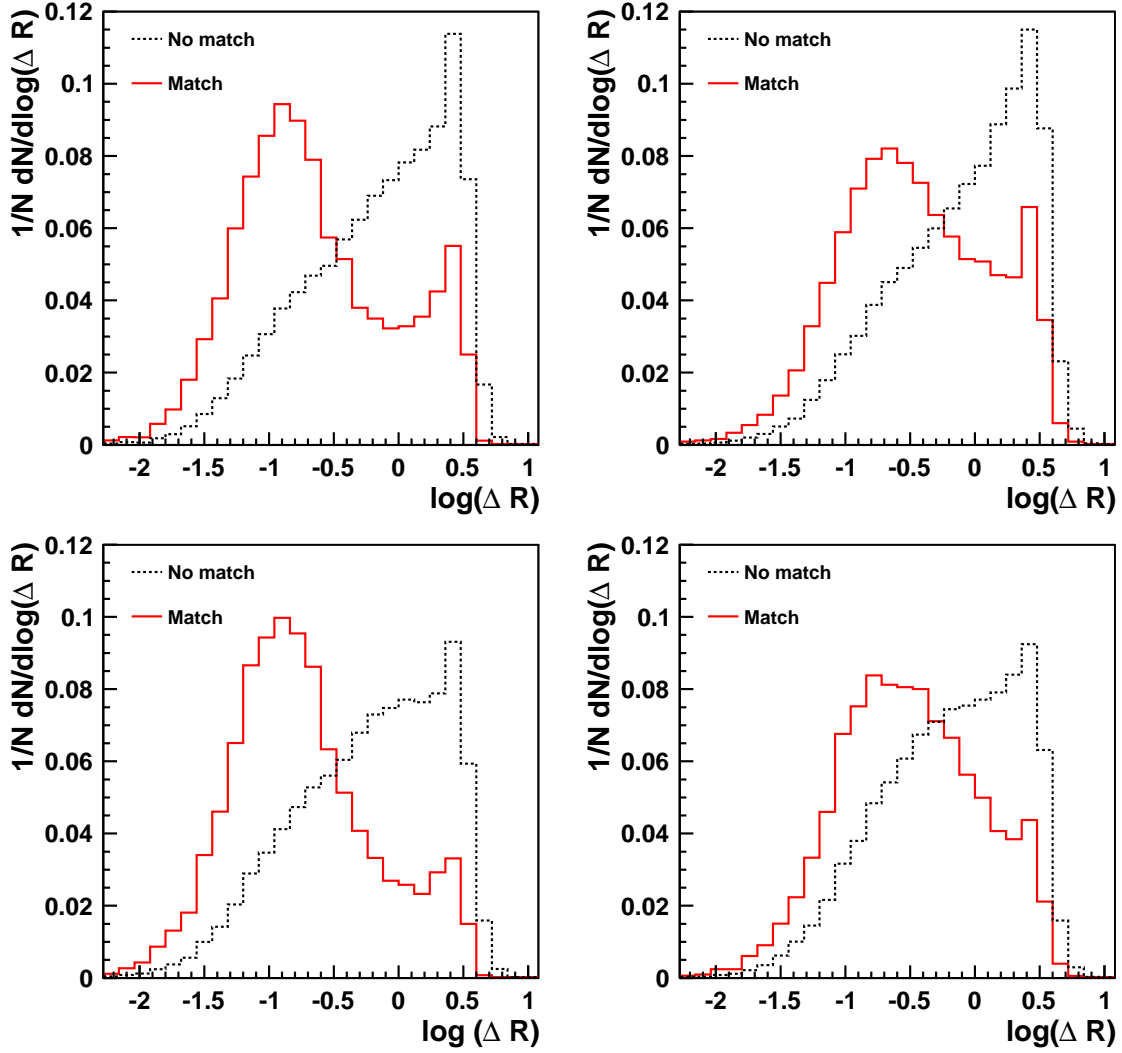


Figure 2: Distance between the true and the direction of the fitted hadronic (left) and leptonic (right) top quark for the best permutation with no constraint on the top mass (top) and with a fixed top pole mass (bottom). Solid line: Matched events, dotted line: No matching requirement. All distributions are normalized to unity.

### 5.3 Reconstructed top masses

For the case that the top pole mass is not fixed it is treated as a free parameter and is estimated during the fitting procedure. Figure 3 shows the distribution of the invariant mass of the three-jet system (left),  $m_{jjj}$ , and of the electron, neutrino and remaining jet-system (right),  $m_{lvj}$ . The distributions have a similar shape due to the small decay width of the top quark. Both extend from 0 to 400  $\text{GeV}/c^2$  and peak at around 170  $\text{GeV}/c^2$ . Further studies on the estimation of the top quark mass are currently being conducted.

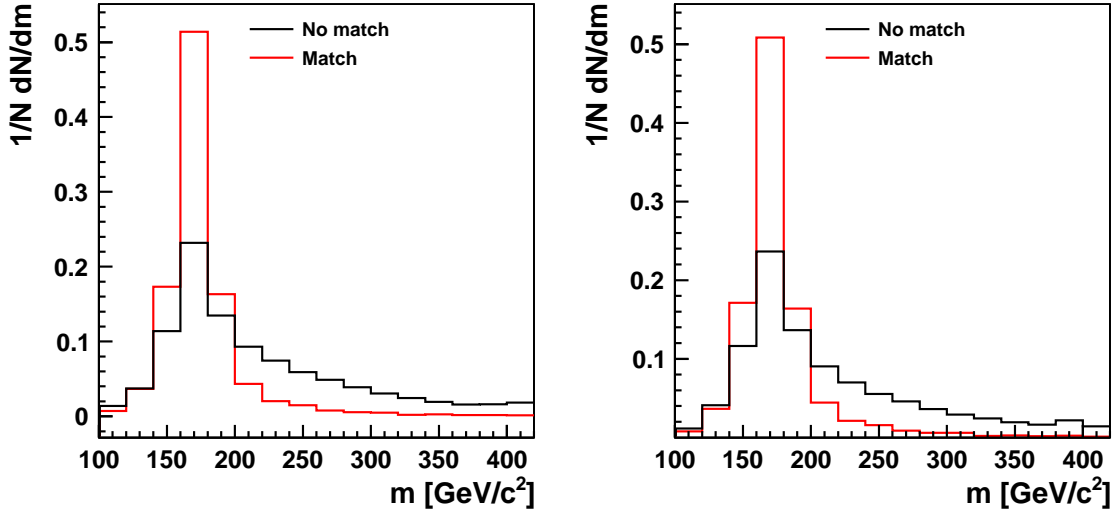


Figure 3: Distribution of the hadronic (left) and leptonic (right) top quark invariant mass for the case of no top pole mass constraint. All distributions are normalized to unity.

### 5.4 Energy resolution

*This part will be written soon.*

## 6 Summary and outlook

A tool for the reconstruction of top quark pairs in semi-leptonic decays has been introduced. The tool is based on a Likelihood approach with an emphasis on the description of the energy resolution of jets and electrons. A study of the performance was conducted on a Monte Carlo data sample. The efficiencies of reconstructing the top quark pair, the hadronically decaying W boson and the b quarks has been deduced. Initial studies on estimating the pole mass of the top quark have been done as well as studies on the energy resolution. These will be continued in the near future.

KLFFitter is available as a stand-alone version [4] and as tool in the ATLAS software framework (TopKLFFitter) [5].

## A Transfer functions

*This part will be written soon.*

## B Control distributions

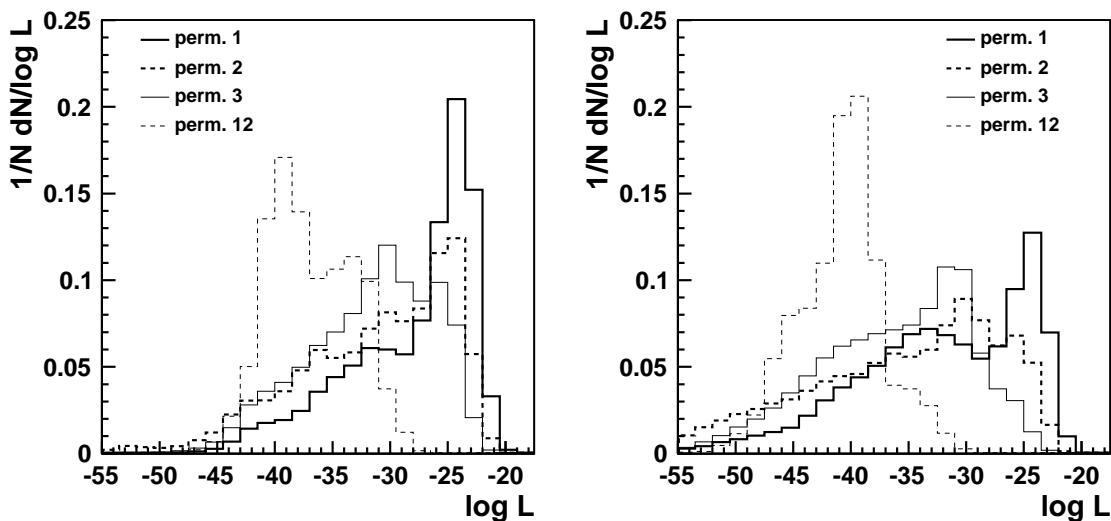


Figure 4: Distribution of the  $\ln L^*$ -values obtained at the mode of the Likelihood for the three best and the worst permutation (left: free top pole mass, right: fixed top pole mass). No matching was required.

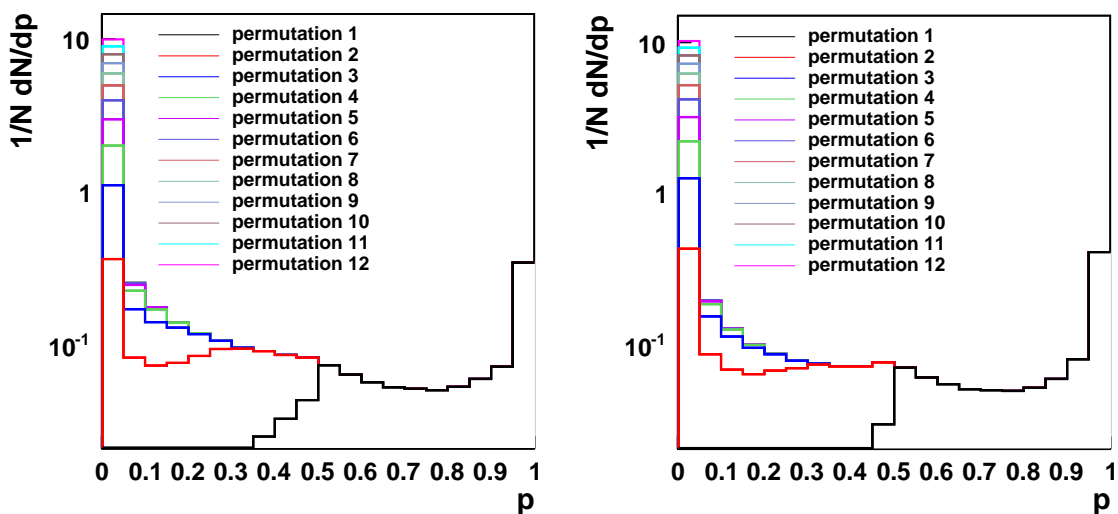


Figure 5: Distribution of the relative weight for all permutations (left: free top pole mass, right: fixed top pole mass). No matching was required.

## References

- [1] For previous studies, see, e.g.,  
M. Stein, K. Kröniger, A. Quadt,  
“Kinematic Fit of  $t\bar{t}$  Events in the Semi-Leptonic Decay Channel with a  $\chi^2$ -Method  
at the ATLAS Experiment,”  
ATL-COM-PHYS-2008-117
- [2] A. Caldwell, D. Kollar and K. Kröniger,  
“BAT - The Bayesian Analysis Toolkit,”  
Comput. Phys. Commun. **180** (2009) 2197 [arXiv:0808.2552].
- [3] G. Aad *et al.* [The ATLAS Collaboration], “Expected Performance of the ATLAS Experiment - Detector, Trigger and Physics,”  
arXiv:0901.0512 [hep-ex].
- [4] Further information on KLFitter can be found at  
<http://physik2.uni-goettingen.de/~kkroeni/KLFitter/>
- [5] Further information on TopKLFitter can be found at  
<https://twiki.cern.ch/twiki/bin/view/AtlasProtected/TopKLFitter>